Journal of Nuclear Materials 389 (2009) 336–340

Contents lists available at ScienceDirect

Journal of Nuclear Materials

journal homepage: www.elsevier.com/locate/jnucmat

# Magnetic order in proton irradiated graphite: Curie temperatures and magnetoresistance effect

J. Barzola-Quiquia, P. Esquinazi, M. Rothermel, D. Spemann *, T. Butz

*Institut für Experimentelle Physik II, Universität Leipzig, Linnéstrasse 5, D-04103 Leipzig, Germany*

A B S T R A C T

Defect induced magnetic order is a new phenomenon in material science that refers to the triggering and manipulation of magnetic order and magnetic moments in nominally non-magnetic materials by lattice defects and/or non-magnetic add atoms. A noticeable example of this effect is the magnetic order at room temperature produced by proton irradiation of graphite. In this work we have managed to increase the ferromagnetic signal by cooling the graphite samples down to 110 K during proton irradiation, diminishing in this way annealing effects. SQUID measurements of the magnetization show a fluence dependent Curie temperature. The longitudinal magnetoresistance shows an irreversible behavior similar to that found in ferromagnetic films indicating spin/domain reorientation effects. The observed magnetoresistance effects and Curie temperatures above room temperature are promising facts that may lead to useful carbon-based devices in the near future.



## 1. Introduction

Magnetic order at room temperature in metal-free carbon-based structures remains one of the exciting issues in fundamental and applied research across all scientific disciplines. However, the lack of reproducibility of early results added to the unknown, in some cases late characterization of the magnetic impurities increased substantially the scepticism of the scientific community. Although there are several theoretical works in the literature on magnetic order in carbon, especially hydrogen induced (see, for example [1] and references cited therein), apart from the proton induced magnetic order in graphite there is not much new systematic experimental work that shows ferromagnetism in metal-free carbon, including in particular a rigorous characterization of the samples impurities. However, there are obstacles that preclude a rush development of this interesting and important subject, e.g., the experimental difficulties to reproduce the magnetic order and the weakness of the ferromagnetic signals, which are sometimes at the limit of the sensitivity of current experimental characterization methods, including SQUID's, as well as annealing effects during ion bombardment, which can hinder the identification of the critical temperature $T_c$ as well as the characteristics and dimensionality of the ferromagnetic signals.

Recent advances in developing nanographitic systems have led to a worldwide renewed interest in their electrical properties [2]. A single layer of graphite, the two-dimensional (2D) graphene, appears to have quantum properties at room temperature [3] as well as rectifying electronic properties [4,5]. The 2D properties of the graphene planes in graphite [6] open up the possibility of using nanometer to micrometer sized regions of graphite in new integrated devices with spintronic properties, through the use of ferromagnetic electrodes, e.g., spin valves, and/or by making graphite itself magnetic.

## 2. Experimental

For our experiments we used five pieces of a HOPG sample ZYA grade (rocking curve width 0.4°), see Table 1. These were irradiated with microspots (μSp; 2.25 MeV proton beam at 1 nA, diameters between 1.2 and 1.7 μm) or spots with a broad beam (BB; 2.0 MeV proton beam at 100 nA, diameter 0.8 mm). All irradiations were performed with the beam perpendicular to the graphite planes. Samples 1–4 were used for the SQUID measurements, whereas the transport properties were measured on sample 5. The spots produced with the microbeam were separated by a distance of 5 μm (sample 1) or 10 μm (samples 2 and 3), similarly to the procedure used in Ref. [7].

The magnetic moment was determined with a superconducting quantum interference device (SQUID) magnetometer from Quantum Design with the reciprocating sample option (RSO) which substantially increases the sensitivity of the magnetization measurements to $\sim 2 \times 10^{-8}$ emu. We note that the SQUID sensitivity without this option is not enough to measure accurately the effects produced by the irradiation, especially when the magnetic signal is of the order of μemu for the saturation ferromagnetic moment. The

* Corresponding author.
*E-mail address:* spemann@physik.uni-leipzig.de (D. Spemann).

0022-3115/$ - see front matter © 2009 Elsevier B.V. All rights reserved.
doi:10.1016/j.jnucmat.2009.02.024

**Table 1**
Irradiation data for the HOPG samples.

| Sample | Mass (mg) | Irradiation type | Temperature | Number of spots | Fluence (nC/μm$^2$) | Total charge (μC) |
|---|---|---|---|---|---|---|
| 1 | 12.8 | μSp | 110 K | 51 375 | 0.69 | 46.9 |
| 2 | 12.5 | μSp | 110 K | 25 600 | 0.77 | 44.8 |
| 3 | 10.1 | μSp | RT | 25 600 | 1.3 | 37.4 |
| 4 | 6 | BB | RT | 6 | 0.3 | 900 |
| 5 | –[a] | BB | RT | 12 | 0.1 | 600 |

RT, room temperature.
[a] The dimensions of sample 5 were 4.4 × 1.5 × 0.01 mm$^3$. μSp: microspots; BB: broad beam; diameter of each spot 0.8 mm.

magnetic field was applied parallel to the graphene planes in all measurements in order to diminish the diamagnetic background.

The resistance measurements were done with a LR700 bridge from Linear Research (with eight channels LR-720 multi-plexer), which has a sensitivity of ⩽10 ppm at the resistances of the selected channels. The resistance was measured using the van der Pauw configuration with a cyclic transposition of current and voltage leads. For the measurements, silver paste electrodes were placed on the sample surface, while the resistance values were obtained in a geometry with an uniform current distribution through the sample cross-section. The magnetic field was continuously swept and monitored with a Hall sensor located near the sample. Here, the measurements were performed in magnetic field parallel to the graphene planes of virgin and irradiated graphite samples for comparison with SQUID results. The temperature stability was better than 0.1 mK. The current applied to the sample was 10 μA and always perpendicular to the applied magnetic field.

## 3. Results and discussion

The samples investigated showed an iron concentration (the only detected magnetic impurity) within the first 35 μm of ∼0.4 ± 0.04 μg/g (<0.1 ppm) as determinated by PIXE measurements. Previous experiments [8] showed ferromagnetic moments at saturation of $m_{sat} \sim 1$ μemu and therefore put severe constraints on the experimentalist, regarding not only the sensitivity of the magnetometer used but also its reproducibility after sample handling. In this work two main experimental improvements have been achieved. First, we enhanced the ferromagnetic part produced by irradiation by reducing annealing effects. In samples 1 and 2 the micrometer spots were produced at a nominal temperature of 110 K during irradiation (18 h). For comparison and to further reduce annealing effects, samples 4 and 5 were irradiated with a broad beam and low fluence. Second, we have designed a sample holder that allows to measure the magnetic moment of the sample in the superconducting quantum interference device (SQUID) as well as to fix it inside the irradiation chamber without any handling of the sample itself. We investigated the reproducibility of the magnetization measurements and checked that the sample holder handling (with sample), i.e., inserting it into and taking it out of the irradiation and SQUID chambers, does not produce systematic changes of the magnetic signal. Our arrangement provides a reproducibility of ∼10$^{-7}$ emu in the measured field range and allows the subtraction of the virgin data from those after irradiation point by point (see Fig. 1).

Fig. 2 shows the hysteresis loops of the magnetic moment $m$ of sample 2 at three temperatures. These loops are obtained directly from the difference of the measurements after and before irradiation. The loop at 5 K as well as the measured temperature dependence at constant field indicate a paramagnetic contribution $m_p = 0.575H/T$ emu K/kOe for this sample, i.e., less than 10% of the ferromagnetic signal at 3 kOe. At 300 K, however, $m_p$ is negligible. These loops and their temperature dependence, as well as the finite

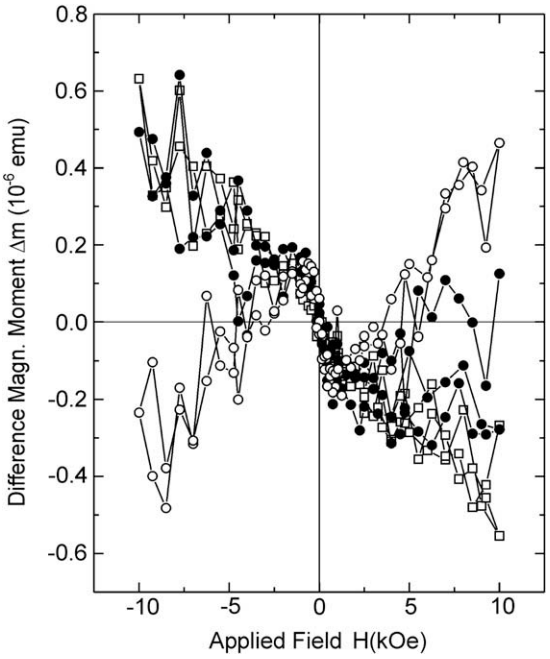


**Fig. 1.** Difference of magnetic moments as a function of field (hysteresis loops) measured for the HOPG sample and holder at four different days at $T = 100$ K. The difference $\Delta m$ is calculated taking the measurement at a certain day as reference. Similar differences are obtained at all temperatures and choosing measurements at other days as reference.

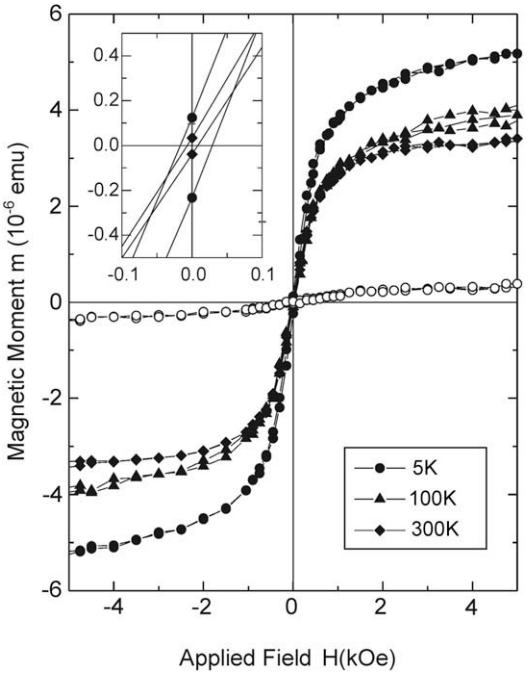


**Fig. 2.** Magnetic moment as a function of applied field for the irradiated sample 2 at 300, 100 and 5 K obtained after subtracting the data for the non-irradiated sample. The open points are obtained for the same sample at 300 K after taking out the first ∼5 μm from the irradiated surface side. The inset blows up the data at low fields to show the finite hysteresis and the clear temperature dependence of the coercive field and the small remanent magnetic moment.

hysteresis, indicate the existence of magnetic order with a Curie temperature higher than room temperature. Sample 3, which was irradiated with a similar number of spots, fluence, and total charge but at room temperature, shows a ferromagnetic signal at saturation

approximately five times smaller than that obtained for samples 1 or 2, in agreement with previous work. These results indicate the reliability and sensitivity of the procedure used as well as the absence of obvious artefacts in the measurements. In order to identify the location of the magnetic contribution from the sample we have removed the first few micrometers from the irradiated surface of sample 2. This reduced the ferromagnetic contribution by one order of magnitude (see open circles in Fig. 2). We can now answer the question of whether the Fe concentration in the sample, due to some hypothetical annealing by the protons, could be responsible for the observed ferromagnetic signal. In the first micrometer depth and, following Ref. [9] and electrostatic force microscopy characterization of sample 2, taking an irradiated magnetic area of ring shape around the centre of the spots of $\leqslant 0.026\ cm^2$, the magnetization at room temperature is $\geqslant 5$ emu/g. In this region we estimate that the mass of the ferromagnetic carbon material is <0.6 μg. Were the measured Fe concentration in this sample region ferromagnetic at 300 K, it would contribute a magnetic moment of $\sim 0.6 \times 10^{-11}$ emu, i.e., $5 \times 10^5$ times smaller than the measured one. Given the mass of the ferromagnetic part of the irradiated HOPG sample, we estimate a magnetic moment per carbon atom of $m_C > \sim 0.01\,\mu_B$, a value consistent with those estimated from X-ray magnetic circular dichroism results [9].

Figs. 3 and 4 show the temperature dependence of the ferromagnetic moment for samples 1 and 4, respectively. Because the paramagnetic signal contributes significantly only at $T \sim 25$ K, we have subtracted it in both figures in order to show only the ferromagnetic part. Up to the highest measured temperature of 380 K, this magnetic moment behaves reversibly. Furthermore, no changes in $m$ within experimental error were observed after leaving the samples for several months at room temperature. One of the interesting and indicative results shown in Figs. 3 and 4 is the unequivocal linear dependence. This is an indication of 2D magnetism, and the slope can be interpreted as due to the excitation of 2D spin waves that reduce the magnetization linearly with $T$.

The discrete Hamiltonian describing the 2D Heisenberg model (2DHM) reads $H = -J\sum_{ij}[S_{iz}S_{jz} + (1-\Delta)(S_{ix}S_{jx} + S_{iy}S_{jy})]$, where $S_i = (S_{ix}, S_{iy}, S_{iz})$ represents a unit vector in the direction of the classical magnetic moment placed at the site $i$ of a 2D lattice. The sum $(i, j)$ is performed over all nearest neighbor pairs, and $J$ is the exchange coupling. The parameter $\Delta$ represents the uniaxial anisotropy in the $z$-direction. The case $\Delta = 0$ is the isotropic 2DHM and is known to have $T_c = 0$. However, just a small anisotropy raises $T_c$ considerably because $T_c \sim -1/\ln\Delta$ for $\Delta \to 0$.

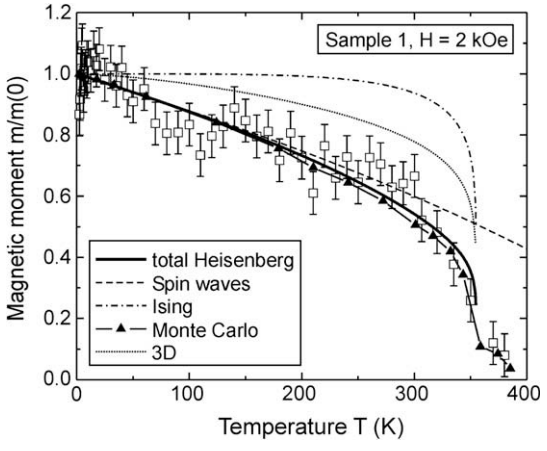


**Fig. 3.** Normalized magnetic moment [$m(0) = 2.60$ μemu] obtained for irradiated sample 1 at 2 kOe. The data points are obtained after subtracting the data from the sample before irradiation and a paramagnetic (Curie) contribution $m_p(T) = 4.9/T$ μemu K. The errors bars indicate typical errors due to the subtraction of the data from the virgin sample. The chosen parameters for the theoretical curves are $T_c = 360$ K, $T_c^{sw} = 850$ K ($\Delta = 0.001$). The continuous line is obtained from Eq. (1). The dotted line is the 3D Bloch $T^{3/2}$ model with spin waves (Ref. [15]). The line with close triangles shows the results of a Monte Carlo simulation with anisotropy (square lattice of 200 × 200 points), see Ref. [10] for more details.

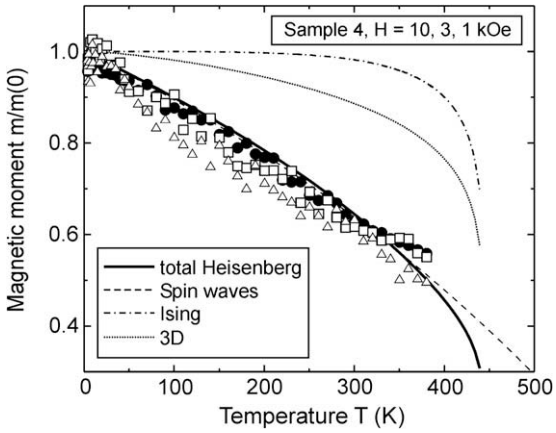


**Fig. 4.** Normalized magnetic moment [$m(0) = 4.9$ μemu at 10 kOe] obtained for sample 4 at 10, 3 and 1 kOe after subtracting the data from the sample before irradiation and a paramagnetic (Curie) contribution $m_p(T) = 1.18H/T$ μemu K/kOe. The different theoretical curves are the same as in Fig. 3 but with parameters $T_c = 450$ K and $T_c^{sw} = 1050$ K [10].

Therefore, to analyze the measured temperature dependence we have to discuss the 2DHM with anisotropy that provides a linear dependence on $T$ [10]. It can be shown [11–13] that the normalized spin wave magnetization in the anisotropic axis behaves as $M_z^{sw} = 1 - T/T_c^{sw} - 2T^2/(T^*T_c^{sw}) - (2/3)(T/T_c^{sw})^3$ at low temperatures, where $T^* = 4J$. The parameter $T_c^{sw}$ is the spin wave critical temperature due to low-energy spin wave excitations; it is given by $k_B T_c^{sw} = 2\pi J/K(1-\Delta)$, where $K(x)$ is the elliptic function. Near the critical temperature $T_c$ the physics can be better described by a 2D Ising model, which should provide a good description of the spin-flip excitations. Then $T_c$ is given by $T_c(\widehat{J}) = 1.52\widehat{J}$ [14], where $\widehat{J}$ is the renormalized exchange due to the spin wave excitations according to the expression $\widehat{J}(T) = J(1 - 2T/T_c^{sw})$. The values of $M_z$ at $T < T_c$ can be expressed as

$$M_z(T) \approx M_z^{sw}(T,J)M_z^{I}[T,\widehat{J}(T)]. \quad (1)$$

The first factor in the right-hand side of (1) is the magnetization due to spin waves, and the second one is the magnetization due to an Ising model with the exchange renormalized by the spin waves. We have checked this theoretical result against Monte Carlo calculations with $\Delta = 0.001$ and the agreement is excellent, especially at low anisotropies [13], as shown in Figs. 3 and 4. In Fig. 3 we have plotted also the normalized spin wave (SW) contribution $M_z^{sw}/M_z^{sw}(0)$ up to third order. The Heisenberg result approximated by (1) and the Monte Carlo calculation agree, and both fit the experimental data with the parameters $T_c^{sw} = 850$ K, $\widehat{J}(T_c = 360\ \text{K}) = 237$ K, indicating an anisotropy $\Delta \approx 0.001$. Sample 2 shows a similar behavior, and its data can be fitted with $T_c^{sw} \approx 1000$ K, $\widehat{J}(T_c \approx 310\ \text{K}) = 202$ K. The data for sample 4 shown in Fig. 4 also show a linear behavior. Extrapolating the SW contribution to $m(T^*) \approx 0$, we conclude that $T_c < T^* \approx 640$ K. Then using (1) we estimate $T_c \geqslant 450$ K with $\Delta \leqslant 10^{-4}$ (see Fig. 4). These results show that $T_c$ decreases with fluence. For comparison we have also plotted in Figs. 3 and 4 the Ising model result, which has no spin waves, and the 3D Bloch $T^{3/2}$ law that includes spin waves [15]. The comparison indicates clearly that spin waves in 2D dominate the magnetization up to 300 K and that the usual 3D model does not fit the data.

Defects in the graphite structure are one of the possible origins for localized magnetic moments. The ferromagnetism triggered by

the bombardment should be correlated to the produced defects located in approximately the first micrometer from the sample surface. To discuss the mechanism responsible for the coupling between the magnetic moments, we need first to estimate the density of defects. For sample 1 we have 0.9 nC total irradiated charge per spot in an area of $\sim\pi 0.6^2$ μm$^2$. Using SRIM2003 Monte Carlo simulations [16] with full damage cascades and 35 eV displacement energy, we obtain a vacancy density of $\sim 5 \times 10^{20}$ cm$^{-3}$ at the surface, which means a distance between vacancies of $l \sim 1.3$ nm $\sim 9a$, where $a = 0.14$ nm. This distance is much smaller than the inverse of the Fermi wave vector $1/k_F \sim 30$ nm for a Fermi energy of 20 meV or that calculated using the 2D carrier density [17–19].

Regarding the coupling needed to have room temperature magnetic ordering, there is in the first place direct coupling for nearly localized spins at the defects, which should be in the range of ~300 K. Recently, Ruderman–Kittel–Kasuya–Yosida (RKKY) coupling between large defects in graphene has been studied for a Fermi energy tending to zero [20]. This coupling might always be ferromagnetic because $k_F r \ll 1$ for $r \sim l$. However, estimations of the Curie temperature for this coupling within our range of defect densities provide values of the order of 20 K. Moreover, recently published work [21] showed that the interaction between defects in graphene is not always ferromagnetic, in contrast to the assumptions done in [20]. What appears important is a super exchange mediated by the two different sites in the graphite lattice [22,23] or between magnetic moments from defects and from hydrogen atoms, which may effectively increase the magnetic moment density on a graphene lattice. We note that a large concentration of hydrogen is found in the region within 1 μm of the surface of graphite samples [24]. Therefore, we should take into account the possible influence of hydrogen in triggering localized as well as non-localized magnetic moments in the graphite layers [22,25]. Irradiation may contribute to defect generation as well as in dissociating the existing molecular hydrogen, enabling its diffusion and bonding in defective parts of the lattice structure. All these moments will tend to be ferromagnetically coupled, enhancing the Curie temperature.

Within this picture, it becomes clear that the enhancement of the defect density which occurs at larger depths from the surface along the ion track up to full amorphization at a depth of ~35–40 μm, perturbs the graphene lattice too much destroying in this way the necessary band structure and carrier density. This may explain the experimental observation of a rather well-defined critical temperature (and not a distribution) and also the difficulty one has in reaching much higher ferromagnetic magnetization values by increasing the proton fluences clearly above the values used here. If an electron-mediated coupling between defects plays a role, we expect that for an adequate defect density it should be possible to influence the magnetic order, shifting the Fermi energy by applying an appropriate bias voltage. The results of samples 1 and 2 provide clear evidence for the good reproducibility of our approach: although the spot density, beam diameter, and total charges were different, the defect densities produced in the irradiated paths were similar for both samples, and therefore we expect to obtain similar critical temperatures, as the measurements showed. By changing the defect density as well as their distribution in the lattice, one may tune the ferromagnetic transition temperature as well as the magnitude of the magnetization produced by irradiation, as the data for sample 4 clearly indicate. As a rule of thumb, robust time dependent ferromagnetism with $T_c > 300$ K can be reached by proton irradiation in graphite with fluences of the order of 0.3 nC/μm$^2$.

After the evidence of magnetic order in HOPG obtained by magnetization measurements using SQUID [10] and magnetic circular X-ray dichroism (XMCD) [9] as well as magnetic force microscopy (MFM) [1] (although this last can be easily overwhelmed by electrostatic forces), an alternative method to detect magnetic ordering is to measure the magnetoresistance and its hysteresis loops. The magnetoresistance is non-hysteretic in case of paramagnetic and diamagnetic samples, but develops a characteristic butterfly loop in case of ferromagnetic samples. This effect derives its strength from the fact that the role of the external field is replaced by an internal field proportional to the magnetization and that the extrema (minima or maxima, depending on the underlying process that changes the resistance with field) in the magnetoresistance appear at the coercive field, when the magnetic induction in the sample vanishes.

Our experimental conditions allow us low-noise transport measurements with ~10 ppm resolution. The magnetoresistance measurements were done in virgin, unirradiated and irradiated samples (sample 5) and for fields parallel to the graphene planes as in the SQUID measurements. For virgin samples there is basically no change of the resistance with parallel magnetic field and no hysteresis in agreement with previous results [26]. After irradiation the situation changes drastically. The results presented here are taken from a ~10 μm thick sample which was irradiated with several 0.8 mm diameter spots that partially overlapped. According to SQUID measurements the ferromagnetic part resides basically in the first micrometers from the surface for the irradiation parameters used and the rest of the sample shows paramagnetic and diamagnetic behavior. Fig. 5(a) shows the ordinary magnetoresistance as a function of field applied parallel to the layers for the irradiated sample 5 at 4 K. Due to the disorder produced by the irradiation the magnetoresistance is negative in the measured field range. A close look at low fields (see Fig. 5(b)) reveals the hysteretic behavior, typical for ferromagnetism, i.e., the minima at the coercive fields

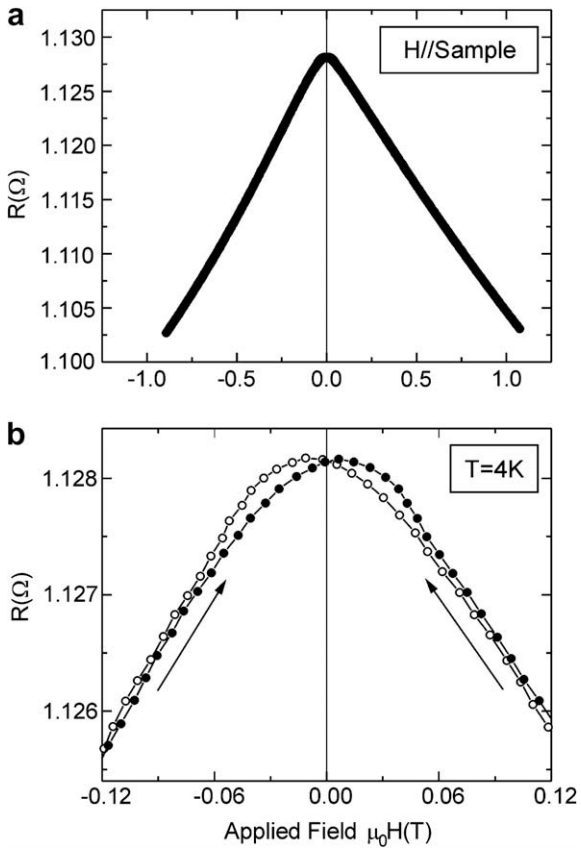


**Fig. 5.** Ordinary magnetoresistance as a function of field applied parallel to the graphene layers for the irradiated sample 5 at 4 K (a). The zoom-in at low fields (b) reveals the hysteretic behavior typical for ferromagnetism.

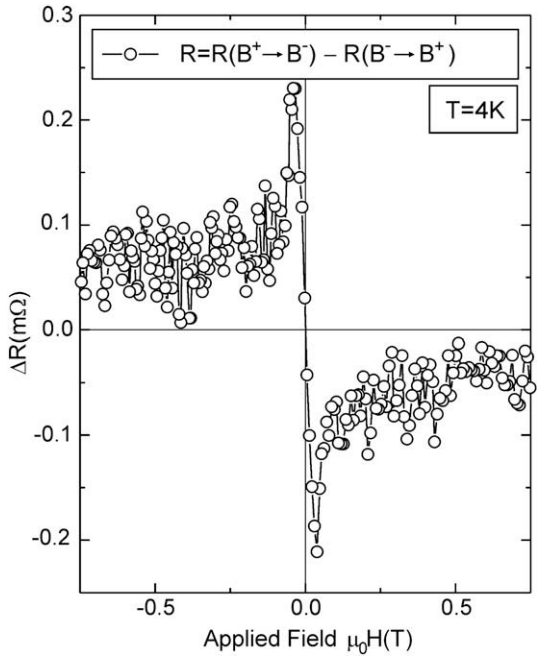


**Fig. 6.** Difference between the resistance measured from positive to negative fields (open circles in Fig. 5(b)) minus the curve obtained in the other field direction (from negative to positive fields, closed circles in Fig. 5(b)). The difference shows hysteresis effects typical for ferromagnetism.

are at the second and fourth quarters of the magnetic field sweep. To enhance the hysteretic behavior, Fig. 6 shows the difference between the resistance measured from positive to negative fields (open circles in Fig. 5(b)) minus the curve obtained in the other field direction (from negative to positive fields, closed circles in Fig. 5(b)). The difference presented in Fig. 6 shows clearly the hysteresis, which combined with Fig. 5(b), leaves no doubt on the ferromagnetic character. Because we measure a sample with a mixture of ferromagnetic and paramagnetic parts in parallel with different absolute values and temperature dependences, the temperature dependence of the ferromagnetic part alone cannot be obtained directly from our measurements. The hysteresis in the magnetoresistance can be observed up to ~20 K. At higher temperatures and due to the decrease of the coercive field as well as of the ferromagnetic magnetic moment the magnetoresistance hysteresis-width decreases below ~10 μΩ (~10 ppm) preventing an accurate measurement of the hysteresis. New experiments on thin samples where the ferromagnetic part should be homogeneously distributed after irradiation are required to obtain the temperature dependence of the magnetoresistance due to ferromagnetism. These experimental difficulties have to be taken into account for future investigations on magnetism in graphite using transport properties.

## 4. Conclusions

In conclusion, our work shows that irradiation of micrometer spots in graphite at low temperatures as well as broad beam irradiation, both at very low fluences, increase significantly the magnitude of the magnetic order with Curie temperatures $T_c \geqslant 300$ K. The use of special sample holders made it possible to reduce sample handling between irradiation chambers and SQUID measurements to a minimum, ruling out simple introduction of impurities or the influence of experimental artifacts. This approach substantially increased the sensitivity and reproducibility of the magnetization measurements, allowing us to obtain directly the effects produced by the irradiation within an error of $\sim 10^{-7}$ emu. The experimental localization of the ferromagnetic irradiated part of the sample indicates that the graphite structure is important, and that at the proton energies used low fluences are preferential to trigger a robust ferromagnetic order. We showed that the magnetization of the magnetically ordered contribution decreases linearly at $T < T_c$, a behavior that can be assigned to the signature of low-energy spin wave excitations well-described by a uniaxial 2D anisotropic Heisenberg model. We have presented first evidence from magneto-transport at low temperature for ferromagnetism in proton irradiated HOPG.

## Acknowledgements

We gratefully acknowledge discussions with N. Garcia. This work was done in the framework of the EU Project 'Ferrocarbon'.

## References

[1] P. Esquinazi, in: H. Kronmüller, S. Parkin (Eds.), Handbook of Magnetism and Advanced Magnetic Materials, vol. 4, John Wiley, Chichester, UK, 2007, p. 2256.
[2] M.I. Katsnelson, Mater. Today 10 (2007) 20.
[3] K.S. Novoselov et al., Science 315 (2007) 1379.
[4] K.S. Novoselov et al., Science 306 (2004) 666.
[5] Y. Zhang, J.P. Small, M.E.S. Amori, P. Kim, Phys. Rev. Lett. 94 (2005) 176803.
[6] Y. Kopelevich, P. Esquinazi, Adv. Mater. 19 (2007) 4559.
[7] K.-H. Han et al., Adv. Mater. (Weinheim, Ger.) 15 (2003) 1719.
[8] P. Esquinazi, D. Spemann, R. Höhne, A. Setzer, K.H. Han, T. Butz, Phys. Rev. Lett. 91 (2003) 227201;
For a recent review see. P. Esquinazi et al., in: T. Makarova, F. Palacio (Eds.), Carbon-Based Magnetism, Elsevier, Amsterdam, 2006, p. 437 (Chapter 19).
[9] H. Ohldag, T. Tyliszczak, R. Höhne, D. Spemann, P. Esquinazi, M. Ungureanu, T. Butz, Phys. Rev. Lett. 98 (2007) 187204.
[10] J. Barzola-Quiquia, P. Esquinazi, M. Rothermel, D. Spemann, T. Butz, N. García, Phys. Rev. B 76 (2007) 161403(R).
[11] W. Doring, Z. Naturforsch. A 16 (1961) 1008.
[12] A.P. Levanyuk, N. García, J. Phys.: Condens. Matter 4 (1992) 10277.
[13] P.A. Serena, N. García, A.P. Levanyuk, Phys. Rev. B 47 (1993) 5027.
[14] E. Brézin, J. Zinn-Justin, Phys. Rev. B 14 (1976) 3110.
[15] C. Kittel, Introduction to Solid State Physics, seventh ed., John Wiley, New York, 1996.
[16] J.F. Ziegler, The Stopping and Range of Ions in Matter, Pregamon Press, New York, 1977.
[17] Y. Kopelevich, J.H.S. Torres, R.R. da Silva, F. Mrowka, H. Kempa, P. Esquinazi, Phys. Rev. Lett. 90 (2003) 156402.
[18] R. Ocaña, P. Esquinazi, H. Kempa, J.H.S. Torres, Y. Kopelevich, Phys. Rev. B 68 (2003) 165408.
[19] H. Kempa, P. Esquinazi, Y. Kopelevich, Solid State Commun. 138 (2006) 118.
[20] M.A.H. Vozmediano, M.P. López-Sancho, T. Stauber, F. Guinea, Phys. Rev. B 72 (2005) 155121.
[21] S. Saremi, Phys. Rev. B 76 (2007) 184430.
[22] O.V. Yazyev, L. Helm, Phys. Rev. B 75 (2007) 125408.
[23] L. Pisani, B. Montanari, N. Harrison, New J. Phys. 10 (2008) 033002.
[24] P. Reichart et al., Nucl. Instrum. Methods Phys. Res. B 249 (2006) 286.
[25] P.O. Lehtinen, A.S. Foster, Y. Ma, A.V. Krasheninnikov, R.M. Nieminen, Phys. Rev. Lett. 93 (2004) 187202.
[26] H. Kempa, H.C. Semmelhack, P. Esquinazi, Y. Kopelevich, Solid State Commun. 125 (2003) 1.